Clinical Neurophysiology 130 (2019) 2193–2202

Contents lists available at ScienceDirect

Clinical Neurophysiology

journal homepage: www.elsevier.com/locate/clinph

The network integration of epileptic activity in relation to surgical outcome

M. Carboni [a,b,*], M. Rubega [b], G.R. Iannotti [a,b,c], P. De Stefano [a], G. Toscano [a,d], S. Tourbier [e], F. Pittau [a], P. Hagmann [e], S. Momjian [c], K. Schaller [c], M. Seeck [a], C.M. Michel [b], P. van Mierlo [a,f], S. Vulliemoz [a,*]

[a] EEG and Epilepsy, Neuroscience Department, University Hospital and Faculty of Medicine of Geneva, Geneva, Switzerland
[b] Functional Brain Mapping Lab, Department of Fundamental Neurosciences, University of Geneva, Geneva, Switzerland
[c] Department of Neurosurgery, University Hospital and Faculty of Medicine of Geneva, Geneva, Switzerland
[d] Unit of Sleep Medicine and Epilepsy, C. Mondino National Neurological Institute, Pavia, Italy
[e] Connectomics Lab, Department of Radiology, University Hospital of Lausanne, Lausanne, Switzerland
[f] Medical Image and Signal Processing Group, Department of Electronics and Information Systems, Ghent University, Ghent, Belgium

ARTICLE INFO

Article history:
Accepted 12 September 2019
Available online 14 October 2019

Keywords:
Epilepsy
Source localization
Connectivity
Network integration
Global efficiency

HIGHLIGHTS

- Abnormal brain network patterns in epilepsy are related to outcome after surgery.
- Lower network integration in patients showing a good post-surgical outcome.
- Isolated activity limits extent of the epileptic network in good outcome patients.

ABSTRACT

Objective: Epilepsy is a network disease with epileptic activity and cognitive impairment involving large-scale brain networks. A complex network is involved in the seizure and in the interictal epileptiform discharges (IEDs). Directed connectivity analysis, describing the information transfer between brain regions, and graph analysis are applied to high-density EEG to characterise networks.
Methods: We analysed 19 patients with focal epilepsy who had high-density EEG containing IED and underwent surgery. We estimated cortical activity during IED using electric source analysis in 72 atlas-based cortical regions of the individual brain MRI. We applied directed connectivity analysis (information Partial Directed Coherence) and graph analysis on these sources and compared patients with good vs poor post-operative outcome at global, hemispheric and lobar level.
Results: We found lower network integration reflected by global, hemispheric, lobar efficiency during the IED ($p < 0.05$) in patients with good post-surgical outcome, compared to patients with poor outcome. Prediction was better than using the IED field or the localisation obtained by electric source imaging.
Conclusions: Abnormal network patterns in epilepsy are related to seizure outcome after surgery.
Significance: Our finding may help understand networks related to a more "isolated" epileptic activity, limiting the extent of the epileptic network in patients with subsequent good post-operative outcome.

1. Introduction

Epilepsy is considered a disorder of neural networks, as reflected by the contribution of multiple cortical and subcortical regions in the expression of seizures and interictal epileptiform discharges (IEDs) with focal or generalized onset. Defining the epileptic network is of great clinical relevance, as structural, electrical, biochemical, or metabolic changes in its components have the capacity to modify seizure and IED expression. The extent of the network involved in focal epileptic activity is not clear, and

Abbreviations: ESI, Electrical Source Imaging; iPDC, Information Partial Directed Coherence; IEDs, interictal epileptiform discharges; LAURA, Local AUtoRegressive Average; LSMAC, Locally Spherical Model with Anatomical Constraints; ROIs, regions of interest; TLE, temporal lobe epilepsy; tv-MVAR, time-varying-multivariate autoregressive.

* Corresponding authors at: EEG and Epilepsy, Neuroscience Department, University Hospital and Faculty of Medicine of Geneva, Geneva, Switzerland (M. Carboni).

E-mail addresses: Margherita.carboni@unige.ch (M. Carboni), Serge.Vulliemoz@unige.ch (S. Vulliemoz).

https://doi.org/10.1016/j.clinph.2019.09.006
1388-2457/

the majority of studies are limited to the exploration of network alterations in temporal lobe epilepsy (TLE) (Laufs and Duncan, 2007). Unique, specific and widespread functional and structural network changes are dependent on the location of focal IEDs and epilepsy type (Fahoum et al., 2012). The relationship between the epileptogenic zone and the seizure onset zone as well as its relationship with remote brain areas can be complex. This might explain why resection of the seizure onset zone only might not always result in seizure freedom.

Electroencephalography (EEG) plays a central role in diagnosis and management of patients with seizure disorders. Electrical Source Imaging (ESI) is an increasingly validated non-invasive approach for localizing the irritative zone and estimating the seizure onset zone in patients with drug-resistant epilepsy undergoing evaluation for surgery (Baroumand et al., 2018; Lascano et al., 2016; Mégevand et al., 2014; Rikir et al., 2014). Nevertheless, other drivers and mechanisms, most likely network-dependent, could influence the post-surgical outcome. Describing and understanding the dynamic mechanisms operating in large-scale human brain networks is likely to produce key insights into epilepsy. EEG-directed functional connectivity analysis in the source space, which describes directionality of information transfer between brain regions, is a promising tool to quantitatively study the pattern of brain connections in epilepsy (Sameshima and Baccala, 2016). In particular, information Partial Directed Coherence (iPDC), a multivariate data-driven method based on the concept of Granger causality has shown its capability to describe epileptic networks. iPDC estimates the direction of information flow between regions considering only direct connections (Astolfi et al., 2007). Once the connections between regions are estimated, the dynamics of global organization of the network can be described using graph theory measures (Sporns et al., 2000). Recent studies showed that such measures of connectivity during physiological activity offer a reliable description of intracortical laminar activity in rodents (Plomp et al., 2014). In humans, graph measures helped in understanding the resting state activity (Coito et al., 2019b) and in differentiating patients with temporal lobe epilepsy from healthy controls (Verhoeven et al., 2018). During IED, dynamic brain network alterations seem related to interictal cognitive deficits (Coito et al., 2015).

In this work, we investigate whether the functional network characteristics estimated using pre-operative high-density EEG and connectivity analysis help predict post-operative outcome after epilepsy surgery. We measured integration properties of the epileptic network using the global efficiency, defined as the ability of a network to combine information. We hypothesize that a more efficient pre-operative epileptic network (as measured by global efficiency), with higher and more widespread communication between brain regions during IEDs, reflects a more extensive epileptic network and is associated with a worse post-surgical outcome.

2. Methods

Database. We selected 19 patients (median age 21 years, range 9–53 y, 11 men) evaluated at the pre-surgical evaluation centre of the epilepsy unit of the Geneva University Hospital and fulfilling the following criteria: (a) pharmacoresistant focal epilepsy with high-density EEG recording with a minimum of 20 unilateral focal IEDs; (b) at least 1-year outcome follow-up after surgery. This study was approved by the local ethics committee.

Patients were classified into good outcome, (ILAE I, Engel Ia (N = 12)) and poor outcome, (ILAE > Ia, Engel > Ia (N = 7)) 0.13 out of 19 (68%) patients had temporal lobe resection (10 of which were good outcome, and 3 poor outcome), the remaining 6/19 (31%) had extra-temporal lobe resection (2 of which were good outcome, and 4 poor outcome). Supplementary Table 1 summarizes the patients' clinical, EEG and imaging details.

EEG acquisition and pre-processing. High-density EEG recordings (128 or 256 electrodes, Electrical Geodesic system, sampling rate = 1000 Hz) were acquired in the context of pre-surgical evaluation at the University Hospital of Geneva. A neurologist with EEG expertise (GPT, MS, FP, and SV) first visually identified and marked IEDs (median across patients 19, range [9:37], (Table 1)). IEDs occurring less than 1-s after a previous IED were not considered to avoid any possible propagation/interference effects of the previous event. Then, 1-s EEG epochs centred on the peak of the marked IED were filtered in the interval [1–40] Hz with a 4th-order Butterworth filter avoiding phase-distortion and down-sampled at 250 Hz. EEG epochs that contained any artefacts surrounding the IEDs were discarded by visual inspection (Fig. 1A). IEDs are well known to be reliable estimators of the seizure onset zone, as they are characterized by higher signal-to-noise ratio and are less contaminated by muscular artefacts compared to ictal events, and finally because IEDs are most likely to be captured during high-density EEG recording sessions (Mégevand et al., 2014).

MRI acquisition and pre-processing. For each patient we created a realistic head model based on the individual structural MRI image, either T1 or MP RAGE, collected during pre-surgical evaluation. Using Freesurfer v6.0.1 and the Connectome Mapper open-source pre-processing software (Daducci et al., 2012), we resampled each image to 1 mm^3 isotropic resolution using cubic interpolation and we performed cortical and subcortical brain parcellation based on Desikan-Killiany (Desikan et al., 2006; Destrieux et al., 2010) anatomical atlas, we kept only parcels accounting for all cortical structures, excluding brainstem, thalamus, and basal ganglia (including nucleus accumbens) structures. This results in a brain parcellation of 72 cortical regions (Fig. 1A).

Scalp level analysis - IED field. A board-certified EEG specialist (SV) qualitatively described the patient-specific IED field as either focal (possibly involving only one lobe), large- field (predominantly one hemisphere) or generalised (simultaneous large-field involvement of both hemisphere) ((Table 1 - 9th column). We compared using a Mann-Whitney U-test ($p < 0.05$) the number of IED analysed between (a) all the patients classified with poor or good post-surgical outcome (b) all the patients with 256 electrodes setup and 129 electrodes setup. We compared using a chi-square ($p < 0.05$) the clinical variables reported (Supplementary Tables 1-2) between the patients classified with poor and good post-surgical outcome.

Source level analysis. According to previous studies, we estimated the maximal source amplitude at 50% of the rising phase since the localization at the peak of the IED is known to be more contaminated by IED propagation (Brodbeck et al., 2011). We tested whether EEG-based analysis, such as the topography of the scalp IED and the localization of the source of maximal power (ESI), could allow the discrimination of good and poor outcomes.

We evaluated the measure of association by computing the phi coefficient (mean squared contingency coefficient) between the outcome of the patient and: (a) the IED field, (b) the concordance between the ESI localization and the clinically defined pathological lobe (in which the resection was performed). The phi coefficient is a modified version of the Pearson correlation for binary variables (a and b), and therefore it can be interpreted as a Pearson correlation.

Inverse space solution. For the forward model, we used a simplified realistic head model with consideration of skull thickness (Locally Spherical Model with Anatomical Constraints (LSMAC)) (Michel and Brunet, 2019) and a grid of around 5000 sources (solution points), distributed equally in the grey matter. Both the lead-field matrix and the inverse matrix were computed using the freely available software Cartool (Michel and Brunet, 2019) and the

Table 1
EEG description: IEDs number and characteristics of each patient. Thick line between patients used to divide good and poor outcome patients.

EEG description				
ID	Number of IED	256 or 129 electrodes	IED characteristics	Concordance ESI and Resection
P1	16	256	focal	No
P2	19	256	focal	Yes
P3	30	256	large field: very active beta activity and spike waves	Yes
P4	25	256	focal and generalised	Yes
P5	9	256	focal	Yes
P6	12	256	focal	Yes
P7	18	256	focal	Yes
P8	20	129	focal	Yes
P9	14	256	focalss	Yes
P10	11	256	focal (also Right Temporal 30%)	Yes
P11	11	256	focal	Yes
P12	11	129	focal very active	Yes
P13	24	256	large field very active	Yes
P14	24	256	focal	Yes
P15	21	256	large field: very active beta activity and spike waves	Yes
P16	29	256	focal	Yes
P17	27	256	focal	Yes
P18	37	129	large field	No
P19	9	129	focal large field	Yes

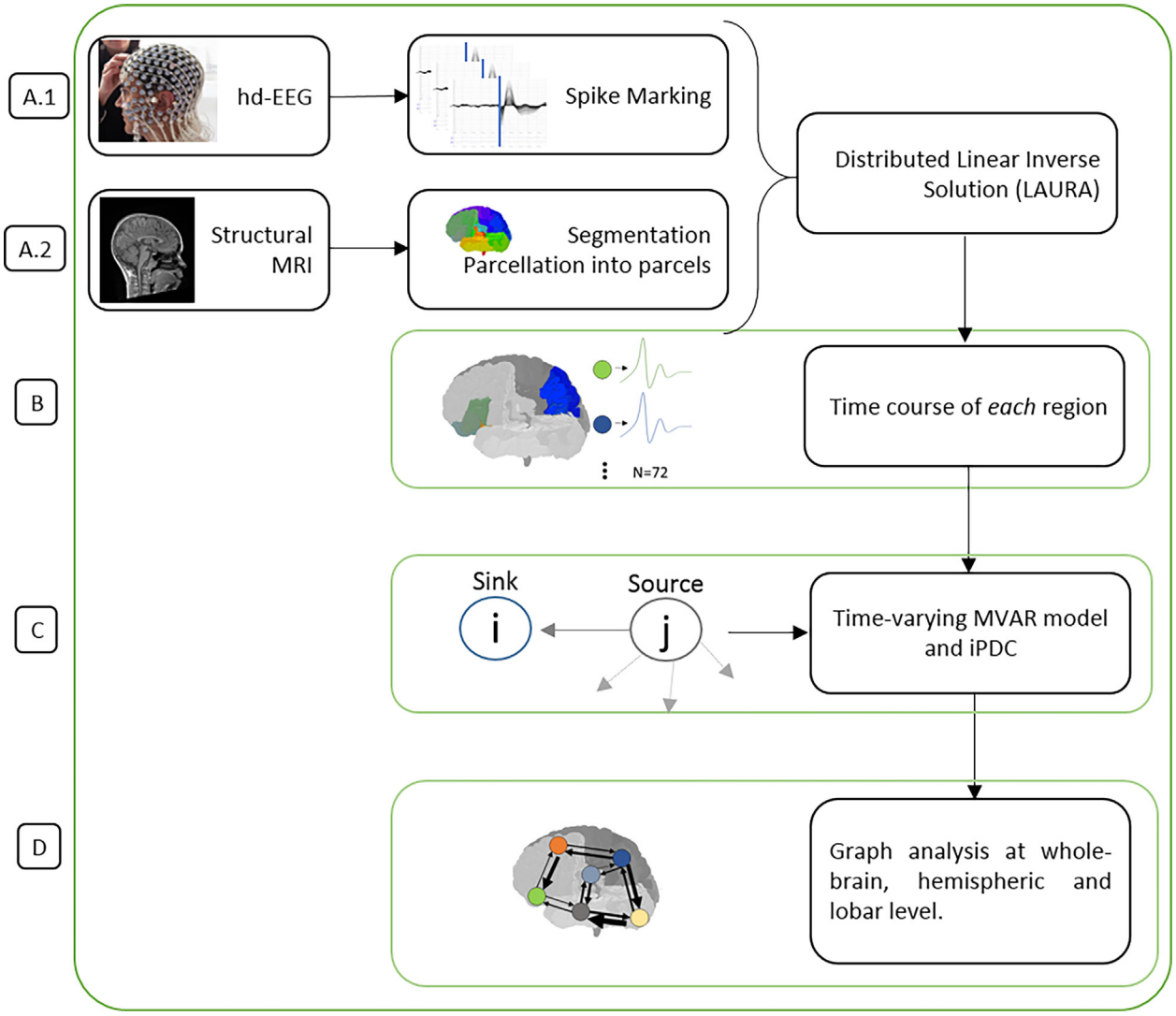

Fig. 1. Summary of the analysis strategy. (A) Around 5000 source-waveforms distributed equally in the grey matter were estimated by a distributed source localization algorithm (LAURA) from the EEG IED. The head model was based on the individual MRI and parcelled into 72 regions of interest (ROI). (B) The activity in each ROI was summarized with a unique time-series through SVD. (C) Connectivity matrices (with time and frequency resolution) were estimated through iPDC. (D) Efficiency was calculated on the entire brain, on the two hemispheres sub-networks and on the eight anatomically defined lobes sub-networks. The connection strengths were compared between different networks (inter hemispheres - inter lobes).

inverse solution performed with LAURA (Local AUtoRegressive Average), one of the state-of-art techniques of distributed inverse solution, which attempts to impose reliable biophysical and physiological constraints to the minimum norm algorithm (Grave De Peralta Menendez et al., 2004) (Fig. 1A). IED-epochs were transformed into source-waveforms at every solution point contained in the 72 regions of interest (ROIs) defined above. In order to sum up the information for each ROI in one time-series, we applied a singular value decomposition-based method (Rubega et al., 2019). As the representative time-series for each region, we considered the first singular vector computed by a singular-value decomposition of all the 3D source-waveform (dipoles) in the same ROI. This signal explains most of the variability of the data content in each ROI (~80%) (Fig. 1B) (Rubega et al., 2019).

Connectivity estimation. In order to deal with non-stationary of the EEG signal, we computed time-varying (tv) connectivity based on the Kalman filter approach for the estimation of high-dimensional tv-multivariate autoregressive (MVAR) models (Milde et al., 2010; Rubega et al., 2019). The model order p, i.e., the maximum time-delay admitted in the model, was constrained at the value of 8, i.e., 28 ms. This value satisfied both the maximum p among all subjects estimated by the Akaike Information Criteria and the hypothesis on the average maximum human brain fibre length (circa 15 cm) and conduction delay (circa 6 m/s) (Caminiti et al., 2013). The value of the forgetting factor of the Kalman filter was constrained at 0.001. Based on visual inspection of the residual of the predictions and the data, we excluded the first 200 ms of each epoch to let the filter adjust to the data. After the estimation of the MVAR coefficients, the connectivity matrices were estimated by applying the information Partial Directed Coherence (iPDC) in the frequency band [1–35] Hz for bins of 0.06 Hz in order to gain resolution on the iPDC matrix. Based on the time-frequency distribution of the power spectral density, this frequency range contains the IED-relevant frequencies (Coito et al., 2016). The magnitude of iPDC was considered for the subsequent analysis.

Eventually, for each patient and for each epoch, we obtained a 4-dimensional matrix ($[\#\ ROIs \times \#\ ROIs \times frequency \times time]$) representing the directed information flow from one ROI to another for each frequency at each time point. The matrix was then averaged across frequencies [1–35 Hz] (Fig. 1C) obtaining a 3-dimensional matrix ($[\#ROIs \times \#ROIs \times time]$) (Fig. 1C).

Graph analysis. In order to extract information from these large connectivity matrices, the brain was represented as a graph defined by a collection of nodes (ROIs) and edges (iPDC directed connections) for each time sample (Fig. 1D). From this graph, we calculated global, hemispheric and lobar network efficiency (Latora and Marchiori, 2001; Rubinov and Sporns, 2010). These measures represent the ability of the network to combine specialized information from distributed brain regions. The local efficiency is defined as the average efficiency of the local subgraphs. The global efficiency can be further estimated by averaging over a given network/sub-network (lobe/hemisphere/whole-brain) [see Appendix A for details]. Since we excluded the first 200 ms of each epoch to let the filter adjust to the data and to get a symmetric epoch around the IED, we evaluated the behaviour of the different types of efficiency over time in a symmetric window between 300 ms before and 300 ms after the peak of the IED. In particular, for each time sample we compared the efficiency values between all the patients classified with poor or good post-surgical outcome using a Mann-Whitney U-test ($p < 0.05$). We furthermore compared the above measures averaged in time in the two different groups. (Fig. 1D).

2.1. Whole brain Efficiency

We constructed a whole brain graph with all the 72 ROIs as nodes and as edges the magnitude of the iPDC values. As described above, we computed the efficiency of the network (Fig. 1D).

2.2. Hemispheric efficiency

We evaluated the hemispheric efficiency by building two subgraphs with nodes in the ipsilateral or in the contralateral hemisphere to the epileptogenic focus. We compared the efficiency of these two sub-networks (ipsilateral vs contralateral hemispheric efficiency) through Mann-Whitney U-test between the two patients' populations (Fig. 1D).

2.3. Hemispheric connections

We divided the inter-hemispheric connections according to the clinical lateralization of the focus in (a) ipsilateral-to-contralateral (b) contralateral-to-ipsilateral. We tested the difference between the two sets of connections (normalized to the total connection strength of each patient) and between the two post-surgical populations through a Mann-Whitney U-test (Fig. 1D).

2.4. Lobar efficiency

Starting from the whole brain iPDC matrix, we constructed eight sub-graphs for each anatomical lobe (left and right frontal, temporal, parietal, and occipital lobe) and we calculated the global efficiency in each lobe (defined as lobar efficiency). Subsequently we compared the lobar efficiency of the eight lobes (Fig. 1D); lobar efficiency values greater than two scaled Median Absolute Deviation (MAD) compared to the median of all other lobes were considered as significant alterations. For each patient we evaluated the number of lobes with altered efficiency (i.e., no lobe, 1 lobe, more than 1 lobe) and the concordance with the clinically defined pathological lobe (subsequently targeted by epilepsy surgery).

2.5. Lobar connections

The inter-lobar connections were defined as: (a) epileptogenic connections: those originating in the clinically defined epileptogenic lobe; (b) other connections: those that started and ended outside of the pathological lobe. We tested the difference between the two types of connections (a and b, both normalized to total connection strength) through a Mann-Whitney U-test for both post-surgical outcomes.

To compute all the above measures, we adapted the functions provided by the freely available Matlab Brain Connectivity toolbox (http://www.brain-connectivity-toolbox.net) (Fig. 1D).

3. Results

3.1. Correlation of the post-surgical outcome with clinical data, IED field, and ESI

None of the tested presurgical clinical and imaging variables were statistically different ($p > 0.05$) in good vs poor post-operative outcome (see Supplementary Table 2). The presence of MRI lesion was tested without other specification. However, we note that hippocampal sclerosis was present only in the good outcome group.

In 9/12 good outcome patients the propagation of the EEG field was defined as focal. In 2/12 good outcome patients the EEG field was defined as large or generalized, in the remaining 1/12 a generalised IED pattern was seen. In 3/7 poor outcome patients the propagation of the EEG field was defined as focal. In 4/7 the EEG field was defined as large. In 11/12 good outcome patients and in 6/7 poor outcome patients the ESI maximum was found concordant with the resection (Table 1). The correlation coefficients between the outcomes and (a) the IED field qualitative description; (b) the ESI maximum concordance in localization with the clinically defined pathological lobe, led to non-significant values ($p > 0.05$ for both analysis). Therefore, the two measures were not sufficient to differentiate groups of patients who were seizure-free after surgery and not. We did not find a significant difference ($p > 0.05$ for both analysis) in the number of IEDs between the good and poor outcome patients and between the two electrodes setup.

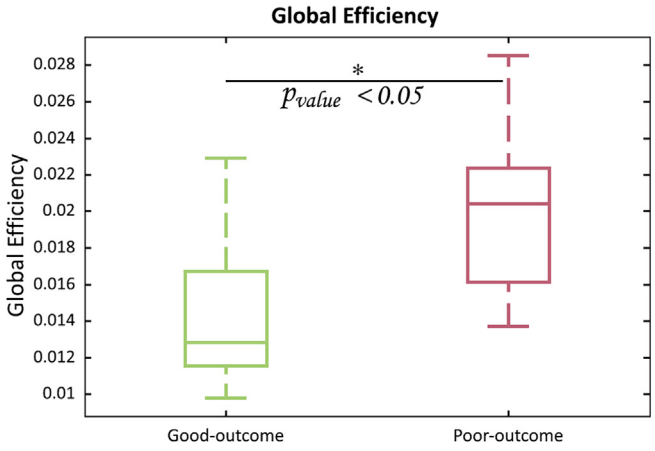

Fig. 2. Boxplot for the values of Global Efficiency across patients with the same outcome, averaged across time. In each box, the central line is the median value, the edges of the boxes are the 75th and the 25th percentiles.

3.2. Efficiency of the entire network

For the entire network, we found a lower pre-operative global efficiency during the IED in patients with subsequent good post-surgical outcome compared to those showing poor post-surgical outcome ($p < 0.05$). This effect was consistent over the duration of the IED, i.e., 600 ms around the peak (Fig. 2).

3.3. Hemispheric evaluation

3.3.1. Hemispheric efficiency

We observed an overall asymmetrical distribution of connectivity strength in patients showing good post-surgical outcome with stronger values in the ipsilateral compared to contralateral hemisphere. However, hemispheric efficiencies calculated on the subnetwork ipsilateral and contralateral to the pathology were not significantly different in both outcome groups ($p > 0.05$). The contralateral hemisphere shows 2 outliers in the good-outcome group (patients P3 and P7). No clear explanation was found for these discordant findings. If these outliers are not considered, contralateral connections in patients showing good post-surgical outcome then show statistically lower efficiency than in the affected hemisphere ($p < 0.05$). The contralateral hemisphere also had significantly lower efficiency in good outcome compared to bad outcome. This effect disappeared if the two outliers were considered in the analysis. In patients showing poor post-surgical outcome, no such trend was observed (Fig. 3).

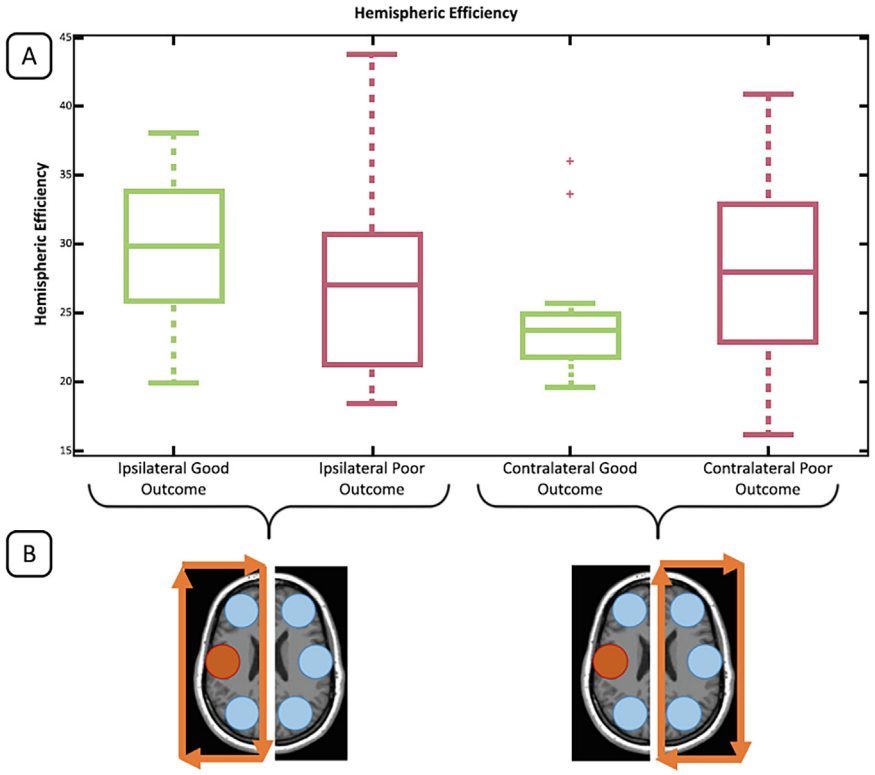

Fig. 3. (A) Boxplot of the strength of connections in patients showing good post-surgical outcome. (B) Schematic representations of the connections, red circles represent the laterality of the epileptic focus. (For interpretation of the references to colour in this figure legend, the reader is referred to the web version of this article.)

3.3.2. Inter-hemisphere connections

In patients showing good post-surgical outcome, the connections starting ipsilateral to the clinically defined pathological lobe were stronger than those starting from the contralateral hemisphere ($p < 0.01$). This difference was not found in patients with poor post-surgical outcome (Fig. 4).

3.4. Lobar evaluation

3.4.1. Lobar efficiency

In 8/12 (67%) patients with good post-surgical outcome, we found only one lobe with significantly higher efficiency, which was overlapping with the clinically defined pathological lobe. In 2/12 (17%) patients, no lobe showed a significant alteration, while for the remaining 2/12 (17%) patients the lobe with higher efficiency was not concordant with the resection. In patients showing poor post-surgical outcome, more than one lobe (including the concordant lobe) (4/7, 57%) or a discordant lobe (3/7, 42%) had abnormally high efficiency; overall patients with good outcome were more likely to show only one lobe with increased efficiency.

For illustration, we show two examples of lobar efficiency values in the eight anatomical lobar networks: one poor outcome (Fig. 5A) and one good outcome (Fig. 5B) patient.

3.4.2. Inter-Lobe connections

In both outcome groups, we found that the inter-lobe connections involving the clinically defined pathological lobe are stronger ($p < 0.05$ for patients showing good and poor post-surgical outcome) as compared with the connections that do not involve the pathological lobe (Fig. 6).

4. Discussion

Our study investigated the dynamic IED-related connectivity patterns in focal epilepsy, to improve our understanding of the complex interplay between pathological areas and whole brain networks during transient interictal epileptic activity. We measured network efficiency at the global, hemispheric and lobar level, to assess how pathological activity is integrated at a large-scale and how this feature could predict post-operative outcome. Differently from previous studies based on icEEG (Bettus et al., 2010; Varotto et al., 2012) our findings are based on scalp EEG, which allows exploring networks at a whole-brain scale as compared to the limited spatial sampling of intracranial electrodes.

4.1. Network integration of pathological activity

Patients in whom the pathological activity affected a smaller part of the brain network had a greater likelihood of good post-surgical outcome compared to those in which the pathological activity affected a more widespread network. This observation was consistent over global and local analyses. On a global "whole-brain" scale, a higher preoperative global efficiency, reflecting more widespread activity, was associated with poor post-operative seizure outcome after focal resection. We interpret this as a lower functional isolation of the epileptic activity (Pedersen et al., 2015), in patients who subsequently do not achieve seizure freedom after surgery allowing a greater extent of the information transfer in the epileptic network. These results were supported by similar findings at the local level: the hemisphere ipsilateral to the presumed epileptogenic zone and the clinically defined pathological lobe show stronger efficiency in the

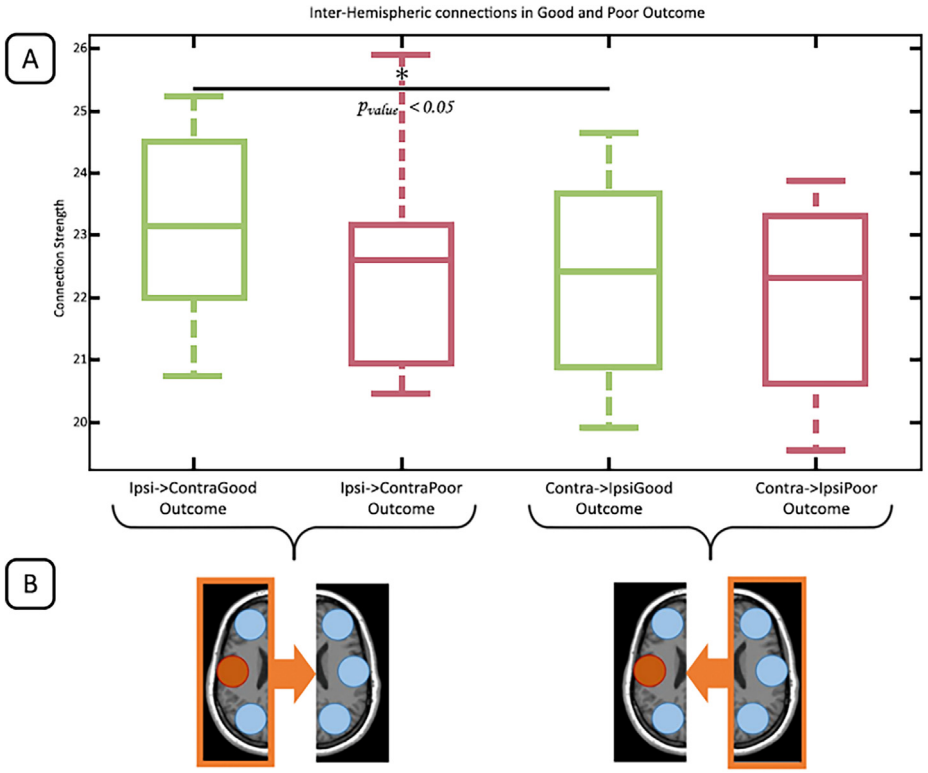

Fig. 4. (A) Boxplot of the strength of connections in patients showing good post-surgical outcome, in green, and in patients showing poor post-surgical outcome, in red. The first and the second boxes from the left represents the strength of the connections from the ipsilateral to the contralateral hemisphere, the third and the fourth boxes represents the strength of the connections from the contralateral to the ipsilateral hemisphere. (B) Schematic representations of the connections, red circles represent the laterality of the epileptic focus. (For interpretation of the references to colour in this figure legend, the reader is referred to the web version of this article.)

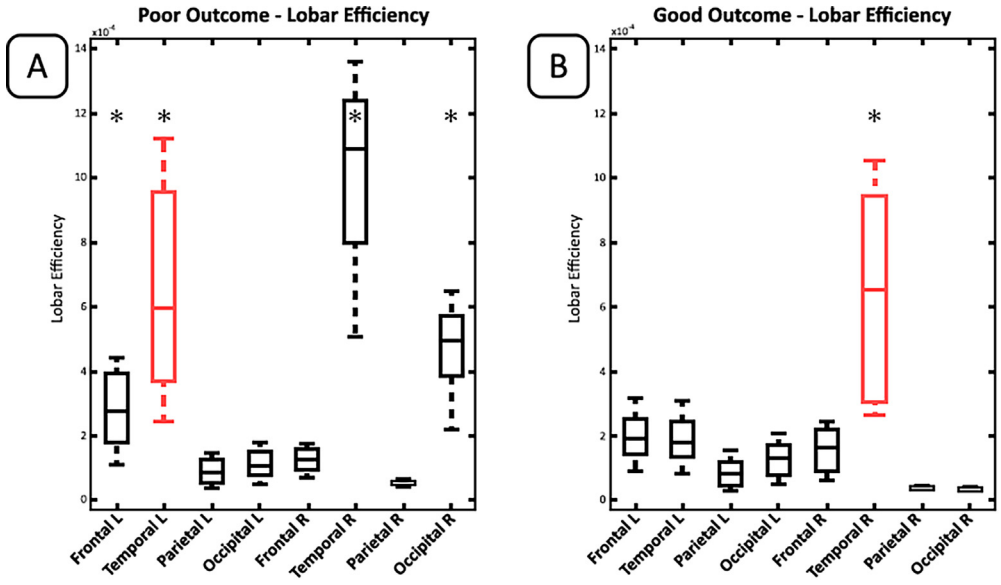

Fig. 5. Boxplots of the values of Global efficiency across time for each lobe in a patient showing poor post-surgical outcome (A) and in a patient showing good post-surgical outcome (B). Red box indicates the lobe with presumed epileptic zone. Stars indicate the lobes with significant increase above 2 MAD. (For interpretation of the references to colour in this figure legend, the reader is referred to the web version of this article.)

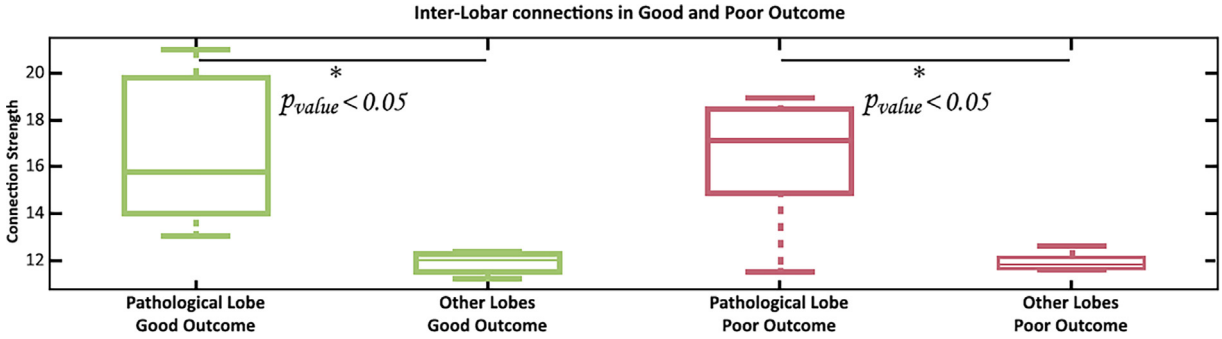

Fig. 6. Strength of connection in patients showing good vs poor post-surgical outcome.

majority of patients showing good post-surgical outcome. At the lobar level, multilobar alterations of efficiency measures were observed in patients with subsequent poor post-operative seizure control. In both outcome groups, the connections involving the epileptogenic lobes were statistically stronger than those that do not involve the pathological lobe. Previous studies using intracranial EEG in focal epilepsy also support the use of direct connectivity as surrogate information for identifying the zone of ictal onset (van Mierlo et al., 2014; Wilke et al., 2011).

Directed connectivity based on Granger modelling offers a different view from icEEG studies that measure synchronization as a measure of 'epileptogenicity'. These studies report increased synchronization within regions involved in the epileptogenic network (Wendling et al., 2010). With our approach, the increased prediction of one ROI activity from the knowledge of past values of another region offers complementary information compared to synchronization. In intracranial EEG studies, stronger interictal connectivity in the regions not involved in the epileptogenic zone was associated with poorer post-operative outcome (Lagarde et al., 2018). This is concordant with our results of poor outcome related to higher global efficiency values in non-operated lobes. These concordant findings may be related to successful vs failed "isolation" of epileptic activity by surrounding inhibitory processes in the interical or ictal conditions (Liou et al., 2018; Muldoon et al., 2015; Schevon et al., 2012).

4.2. Clinical relevance of EEG-based network imaging

Electromagnetic source imaging using EEG or MEG to localize the irritative zone is increasingly validated as a clinical tool and a reliable surrogate for localizing the seizure onset zone (using icEEG validation) (Mégevand et al., 2014) and the epileptic zone (EZ) (using post-operative outcome) (Brodbeck et al., 2011; Englot et al., 2015; Lascano et al., 2016; Rikir et al., 2014; Sharma et al., 2018). Therefore, the clinical relevance of network imaging based on EEG is probably not so much to improve such localization, but rather to inform about large-scale abnormal connectivity that may offer additional information for diagnosis and prognosis in epilepsy. A single focus may not be the best way of understanding the pathophysiology underlying seizure and IEDs activity (van Mierlo et al., 2014) and being able to distinguish which of the nodes initiates abnormal behaviour may not be sufficient for an accurate analysis of the epileptic network. The directed connectivity measure and the evaluation of the connections between nodes could be informative in detecting additional clinically meaningful network properties (Coito et al., 2016). Indeed, different brain areas acting as a network with imbalance between excitatory and inhibitory mechanisms may promote epileptic activity, and the pattern of involvement of multiple brain regions in the epileptogenic network could affect the surgical outcome. We showed that patients with good outcome after surgery gener-

ally have the strongest alteration localized in the pathological lobe concordant with the resection together with a predominantly ipsilateral alteration of connections, while poor outcome patients show more widespread alterations both within and outside the pathological lobe. In our patient group, these connectivity alterations were superior to predict post-operative outcome compared to other EEG markers, such as the number of IED, focality of IED or the localisation of the source. This comparison in the same patient group, despite its small size, offers additional support for the added value of connectivity measures as a clinical tool. In addition, some widely accepted predictors of a worse outcome may also be indirect markers of a more widespread epileptogenic network. Indeed, longer disease duration, history of generalised tonic-clonic seizures or learning disability have all been associated with lower post-operative seizure control (Bell et al., 2017). Our findings of increased efficiency related to poor post-operative outcome is also concordant with impaired ipsilateral connectivity and increased contralateral functional connectivity observed with fMRI studies although these studies focused on interictal activity without IED or irrespective of the presence of IED. Increased hemispheric connectivity is a strong indicator of focus lateralization (Bettus et al., 2010). In another study, a lower lateralisation of connections seeded from the presumed EZ (i.e. a stronger connectivity to the contralateral hemisphere), was associated with a poorer post-operative seizure outcome (Negishi et al., 2011). Scalp EEG-based connectivity analysis in the absence of IED would be crucial to compare resting state connectivity patterns across imaging modalities.

Directed connectivity also showed promising results for non-invasive localization of the ictal onset zone based on high-density EEG (Ding et al., 2009; Staljanssens et al., 2017a), or low-density long-term clinical recordings (Staljanssens et al., 2017b).

4.3. Methodological considerations

The scalp-EEG analysis is affected by two major limitations that can influence connectivity estimation: the volume conduction problem (i.e., each EEG channel can be considered as a linear mixture of concurrently active brain and non-brain electrical sources whose activities are volume conducted to the scalp electrodes) and the EEG reference problem (i.e., the signal in each electrode is obtained as the difference between the electric potentials in its location and in the location of the reference electrode). These properties are particularly relevant in connectivity analyses, which aim to detect the real active interactions between brain regions. Connectivity analysis performed in the *source space* is able to partially overcome these issues (Schoffelen and Gross, 2009). PDC estimations do not consider zero-lag interactions that describe the instantaneous propagation of activity, whereas the reference problem that heavily influences the sensor space analysis, does not affect the source-reconstructed signal, which is reference-free (Michel et al., 2009).

In this study, we applied iPDC to our data to estimate directed measures of connectivity (Hassan et al., 2014). Directed connectivity measures based on Granger causal modelling have shown physiological and clinical relevance in a growing number of studies. They have been initially validated in simulation studies (Astolfi et al., 2005) and animal models(Plomp et al., 2014), then applied to intra-cranial EEG recordings of patients with epilepsy during IED (interictal) (Chan et al., 2012), preictal (Varotto et al., 2012) and ictal conditions (Van Mierlo et al., 2011). In temporal lobe epilepsy, IED-related connectivity patterns based on scalp high-density EEG were concordant with the epileptogenic zone (Coito et al., 2015, 2019a) and with cognitive deficits (Coito et al., 2015). Directed connectivity analyses have also shown that the "resting-state" EEG network is concordant with fMRI observations on the default mode network in healthy subjects and patients with temporal lobe epilepsy (Coito et al., 2019b). However, in patients affected by temporal lobe epilepsy, the main connectivity drivers were different compared to healthy controls, allowing an accurate classification at single subject level (Coito et al., 2016; Verhoeven et al., 2018). A simulation study comparing several methods to compute the inverse solution and connectivity has suggested that the undirected phase lag index approach combined with minimum norm estimation had highest accuracy compared to weighted minimum norm or low resolution brain electromagnetic tomography (LORETA), but this finding has not been tested yet in a significant group of patients (Hassan et al., 2014). Larger studies are warranted to compare connectivity approaches applied to interictal (IED and non-spiking data) as well as ictal recordings, in order to gain deeper insight into the diagnostic and prognostic values of all these different strategies in estimating the pathological brain network.

It should be taken into account that the relatively small sample size and the heterogeneous nature of epilepsy limit the analysis between groups. For instance, hippocampal sclerosis was present only in the good outcome group. Nevertheless, other temporal lesions with usual good outcome were also found in the poor outcome group strengthening the view that clinical variable alone cannot completely predict outcome and that additional markers, such as connectivity, are needed. We encountered the problem of obtaining high-density EEG recording with a sufficient number of IEDs for a reliable estimation of the multivariate coefficients for the connectivity analysis. We have also to keep in mind that these events are strongly related to the epileptogenic zone in most cases. Further studies of connectivity alterations in EEG segments without IEDs would be interesting for predicting epilepsy surgery outcome, but also more broadly, for assessing seizure risk in brain disorders, confirming or classifying epilepsy diagnosis in difficult cases and predicting the response to medical treatment. A broader applicability could be envisaged for other disorders.

5. Ethical publication statement

We confirm that we have read the Journal's position on issues involved in ethical publication and affirm that this report is consistent with those guidelines.

Due to data protection reasons, data cannot be made publicly available. However, anonymized grouped data will be made available upon reasonable request to qualified investigators.

Acknowledgements

This work was supported by the Swiss National Science Foundation (SNSF) [under grants CRSII5_170873 and 169198]. Author M.S. was supported by SNSF 163398 and Sinergia 180365. Part of this work was performed within the FLAG-ERA/JTC 2017 "SCALES" project.

The Cartool software (http://sites.google.com/site/fbmlab/cartool) has been programmed by Denis Brunet from the Functional Brain Mapping Laboratory in Geneva and is supported by the Center for Biomedical Imaging (CIBM) of Geneva and Lausanne, Switzerland.

Declaration of Competing Interest

PvM is a co-founder and shareholder of Epilog NV (Ghent, Belgium). MS and SV are advisors and shareholders of Epilog NV (Ghent, Belgium). None of the other authors has any conflict of interest to disclose.

Appendix A. Network measures

Local efficiency is defined as the average efficiency of the local subgraphs (Latora and Marchiori 2001). This quantity reveals how much the system is fault tolerant, i.e., it shows how efficient the communication is between the first neighbours of i when i is removed.

$$\overrightarrow{E_{loc}} = \frac{1}{2n}\sum_{i\in N}\frac{\sum_{j,h\in N, j\neq i}(a_{ij}+a_{ji})(a_{ih}+a_{hi})(\left[\overrightarrow{d_{jh}}(N_i)\right]^{-1}+\left[\overrightarrow{d_{hj}}(N_i)\right]^{-1})}{\left(k_i^{out}+k_i^{in}\right)\left(k_i^{out}+k_i^{in}-1\right)-2\sum_{j\in N}a_{ij}a_{ji}} \tag{A1}$$

where k_i^{out} is the out-degree of node i, k_i^{in} is the in-degree of node i, and a_{ij} is the connection status between i and j, i.e., $a_{ij}=1$ if the link between i and j exists, $a_{ij}=0$ otherwise. N is the set of nodes in the network. n is the number of nodes and $\overrightarrow{d_{jh}}(N_i)$ is the length of the shortest directed path between $j$and h that contains only neighbours of i.

Global efficiency evaluates the ability of the brain to rapidly combine specialized information from distributed brain regions. The global efficiency measures the inverse of the shortest path length. Structural network usually are similarly organized and share a high global efficiency whereas functional network have weaker connections between modules and consequently a weaker global efficiency (Honey et al., 2007).

$$\overrightarrow{E} = \frac{1}{n}\sum_{i\in N}\frac{\sum_{j\in N, j\neq i}\left(\overrightarrow{d}_{ij}\right)^{-1}}{n-1} \tag{A2}$$

Appendix B. Supplementary data

Supplementary data to this article can be found online at https://doi.org/10.1016/j.clinph.2019.09.006.

References

Astolfi L, Cincotti F, Mattia D, Babiloni C, Carducci F, Basilisco A, et al. Assessing cortical functional connectivity by linear inverse estimation and directed transfer function: Simulations and application to real data. Clin Neurophysiol 2005;116:920–32.

Astolfi L, Cincotti F, Mattia D, Marciani MG, Baccala LA, Fallani FDV, et al. Comparison of different cortical connectivity estimators for high-resolution EEG recordings. Hum Brain Mapp 2007;28:143–57.

Baroumand AG, van Mierlo P, Strobbe G, Pinborg LH, Fabricius M, Rubboli G, et al. Automated EEG source imaging: A retrospective, blinded clinical validation study. Clin Neurophysiol 2018;129:2403–10.

Bell GS, De Tisi J, Gonzalez-Fraile JC, Peacock JL, McEvoy AW, Harkness WFJ, et al. Factors affecting seizure outcome after epilepsy surgery: An observational series. J Neurol Neurosurg Psychiatry 2017;88:933–40.

Bettus G, Bartolomei F, Confort-Gouny S, Guedj E, Chauvel P, Cozzone PJ, et al. Role of resting state functional connectivity MRI in presurgical investigation of mesial temporal lobe epilepsy. J Neurol Neurosurg Psychiatry 2010;81:1147–54.

Brodbeck V, Spinelli L, Lascano AM, Wissmeier M, Vargas MI, Vulliemoz S, et al. Electroencephalographic source imaging: A prospective study of 152 operated epileptic patients. Brain 2011;134:2887–97.

Caminiti R, Carducci F, Piervincenzi C, Battaglia-Mayer A, Confalone G, Visco-Comandini F, et al. Diameter, length, speed, and conduction delay of callosal axons in macaque monkeys and humans: comparing data from histology and magnetic resonance imaging diffusion tractography. J Neurosci 2013;33:14501–11.

Chan HL, Tsai YT, Wang YC, Ju JH, Chang BL, et al.. Partial directed coherence analysis of intracranial neural spikes in epilepsy patients. Proc Annu Int Conf IEEE Eng Med Biol Soc EMBS Int Conf IEEE Eng Med Biol Soc EMBS; 2012. p. 5174–77.

Coito A, Biethahn S, Tepperberg J, Carboni M, Roelcke U, Seeck M, et al. Interictal epileptogenic zone localization in patients with focal epilepsy using electric source imaging and directed functional connectivity from low-density EEG. Epilepsia Open 2019a;4.

Coito A, Genetti M, Pittau F, Iannotti GR, Thomschewski A, Höller Y, et al. Altered directed functional connectivity in temporal lobe epilepsy in the absence of interictal spikes: A high density EEG study. Epilepsia 2016;57:402–11.

Coito A, Michel CM, Vulliemoz S, Plomp G. Directed functional connections underlying spontaneous brain activity. Hum Brain Mapp 2019b;40:879–88.

Coito A, Plomp G, Genetti M, Abela E, Wiest R, Seeck M, et al. Dynamic directed interictal connectivity in left and right temporal lobe epilepsy. Epilepsia 2015;56:207–17.

Daducci A, Gerhard S, Griffa A, Lemkaddem A, Cammoun L, Gigandet X, et al. The Connectome Mapper: An Open-Source Processing Pipeline to Map Connectomes with MRI. PLoS One 2012;7.

Desikan RS, Ségonne F, Fischl B, Quinn BT, Dickerson BC, Blacker D, et al. An automated labeling system for subdividing the human cerebral cortex on MRI scans into gyral based regions of interest. Neuroimage 2006;31:968–80.

Destrieux C, Fischl B, Dale A, Halgren E. Automatic parcellation of human cortical gyri and sulci using standard anatomical nomenclature. Neuroimage 2010;53:1–15.

Ding L, Wilke C, Xu B, Xu X, Van Drongelene W, He B. EEG source imaging: correlate source locations and extents with ECoG and surgical resections in epilepsy patients. J Clin Neurophysiol 2009;24:130–6.

Englot DJ, Nagarajan SS, Imber BS, Raygor KP, Honma SM, Mizuiri D, et al. Epileptogenic zone localization using magnetoencephalography predicts seizure freedom in epilepsy surgery. Epilepsia 2015;56:949–58.

Fahoum F, Lopes R, Pittau F, Dubeau F, Gotman J. Widespread epileptic networks in focal epilepsies: EEG-fMRI study. Epilepsia 2012;53:1618–27.

Grave De Peralta Menendez R, Murray MM, Michel CM, Martuzzi R, Gonzalez Andino SL. Electrical neuroimaging based on biophysical constraints. Neuroimage 2004;21:527–39.

Hassan M, Dufor O, Merlet I, Berrou C, Wendling F. EEG source connectivity analysis: From dense array recordings to brain networks. PLoS One 2014;9.

Honey CJ, Kötter R, Breakspear M, Sporns O. Network structure of cerebral cortex shapes functional connectivity on multiple time scales. PNAS 2007;104:10240–5.

Lagarde S, Roehri N, Lambert I, Trebuchon A, McGonigal A, Carron R, et al. Interictal stereotactic-EEG functional connectivity in refractory focal epilepsies. Brain 2018;141:2966–80.

Lascano AM, Perneger T, Vulliemoz S, Spinelli L, Garibotto V, Korff CM, et al. Yield of MRI, high-density electric source imaging (HD-ESI), SPECT and PET in epilepsy surgery candidates. Clin Neurophysiol 2016;127:150–5.

Latora V, Marchiori M. Efficient Behavior of Small-World Networks. Phys Rev Lett 2001;87:3–6.

Laufs H, Duncan JS. Electroencephalography/functional MRI in human epilepsy: What it currently can and cannot do. Curr Opin Neurol 2007;20:417–23.

Liou JY, Ma H, Wenzel M, Zhao M, Baird-Daniel E, Smith EH, et al. Role of inhibitory control in modulating focal seizure spread. Brain 2018;141:2083–97.

Mégevand P, Spinelli L, Genetti M, Brodbeck V, Momjian S, Schaller K, et al. Electric source imaging of interictal activity accurately localises the seizure onset zone. J Neurol Neurosurg Psychiatry 2014;85:38–43.

Michel CM, Brunet D. EEG Source Imaging : a practical review of the analysis steps. Front Neurol 2019;10:1–36.

Michel CM, Koenig T, Brandeis D, Gianotti L, Wackermann J. Electrical Neuroimaging. Cambridge University Press; 2009.

Van Mierlo P, Carrette E, Hallez H, Vonck K, Van Roost D, Boon P, et al. Accurate epileptogenic focus localization through time-variant functional connectivity analysis of intracranial electroencephalographic signals. Neuroimage 2011;56:1122–33.

van Mierlo P, Papadopoulou M, Carrette E, Boon P, Vandenberghe S, Vonck K, et al. Functional brain connectivity from EEG in epilepsy: Seizure prediction and epileptogenic focus localization. Prog Neurobiol 2014;121:19–35.

Milde T, Leistritz L, Astolfi L, Miltner WHR, Weiss T, Babiloni F, et al. A new Kalman filter approach for the estimation of high-dimensional time-variant multivariate AR models and its application in analysis of laser-evoked brain potentials. Neuroimage 2010;50:960–9.

Muldoon SF, Villette V, Tressard T, Malvache A, Reichinnek S, Bartolomei F, et al. GABAergic inhibition shapes interictal dynamics in awake epileptic mice. Brain 2015;138:2875–90.

Negishi M, Martuzzi R, Novotny EJ, Spencer DD, Constable RT. Functional MRI connectivity as a predictor of the surgical outcome of epilepsy. Epilepsia 2011;52:1733–40.

Pedersen M, Omidvarnia AH, Walz JM, Jackson GD. Increased segregation of brain networks in focal epilepsy: An fMRI graph theory finding. NeuroImage Clin 2015;8:536–42.

Plomp G, Quairiaux C, Michel CM, Astolfi L. The physiological plausibility of time-varying Granger-causal modeling: Normalization and weighting by spectral power. Neuroimage 2014;97:206–16.

Rikir E, Koessler L, Gavaret M, Bartolomei F, Colnat-Coulbois S, Vignal JP, et al. Electrical source imaging in cortical malformation-related epilepsy: A prospective EEG-SEEG concordance study. Epilepsia 2014;55:918–32.

Rubega M, Carboni M, Seeber M, Pascucci D, Tourbier S, Toscano G, et al. Estimating EEG Source Dipole Orientation Based on Singular-value Decomposition for Connectivity Analysis. Brain Topogr 2019;32:704–19.

Rubinov M, Sporns O. Complex network measures of brain connectivity: Uses and interpretations. Neuroimage 2010;52:1059–69.

Sameshima K, Baccala LA. Methods in Brain Connectivity Inference through Multivariate Time Series Analysis. CRC Press; 2016.

Schevon CA, Weiss SA, McKhann G, Goodman RR, Yuste R, Emerson RG, et al. Evidence of an inhibitory restraint of seizure activity in humans. Nat Commun 2012;3:1011–60.
Schoffelen JM, Gross J. Source connectivity analysis with MEG and EEG. Hum Brain Mapp 2009;30:1857–65.
Sharma A, Rai JK, Tewari RP. Epileptic seizure anticipation and localisation of epileptogenic region using EEG signals. J Med Eng Technol 2018;42:203–16.
Sporns O, And GT, Edelman GM. Theoretical Neuroanatomy: Relating Anatomical and Functional Connectivity in Graphs and Cortical Connection Matrices. Cereb Cortex 2000;10:127.
Staljanssens W, Strobbe G, Van Holen R, Birot G, Gschwind M, Seeck M, et al. Seizure Onset Zone Localization from Ictal High-Density EEG in Refractory Focal Epilepsy. Brain Topogr 2017a;30:257–71.
Staljanssens W, Strobbe G, Van Holen R, Keereman V, Gadeyne S, Carrette E, et al. EEG source connectivity to localize the seizure onset zone in patients with drug resistant epilepsy. NeuroImage Clin 2017b;16:689–98.
Varotto G, Tassi L, Franceschetti S, Spreafico R, Panzica F. Epileptogenic networks of type II focal cortical dysplasia: A stereo-EEG study. Neuroimage 2012;61:591–8.
Verhoeven T, Coito A, Plomp G, Thomschewski A, Pittau F, Trinka E, et al. Automated diagnosis of temporal lobe epilepsy in the absence of interictal spikes. NeuroImage Clin 2018;17:10–5.
Wendling F, Chauvel P, Biraben A, Bartolomei F. From Intracerebral EEG Signals to Brain Connectivity: Identification of Epileptogenic Networks in Partial Epilepsy. Front Syst Neurosci 2010;4:1–13.
Wilke C, Worrell G, He B. Graph analysis of epileptogenic networks in human partial epilepsy. Epilepsia 2011;52:84–93.